Direct measurement of *Mycobacterium*–fibronectin interactions

Claire Verbelen and Yves F. Dufrêne*

Bacterial surface-associated proteins play essential roles in mediating pathogen–host interactions and represent privileged targets for anti-adhesion therapy. We used atomic force microscopy (AFM) to investigate, *in vivo*, the binding strength and surface distribution of fibronectin attachment proteins (FAPs) in *Mycobacterium bovis bacillus* Calmette-Guérin (BCG). We measured the specific binding forces of FAPs ($\sim$50 pN) and found that they increased with the loading rate, as observed earlier for other receptor–ligand systems. We also mapped the distribution of FAPs, revealing that the proteins are widely exposed on the mycobacterial surface. To demonstrate that the proteins are surface-associated, we showed that treatment of the cells with pullulanase, an enzyme possessing carbohydrate-degrading activities, or with protease, an enzyme that conducts proteolysis, led to a substantial reduction of the FAP surface density. A similar trend was also noted following treatment with ethambutol, an antibiotic which inhibits the synthesis of cell wall polysaccharides. The nanoscale analyses presented here complement traditional proteomic and molecular biology approaches for the functional analysis of surface-associated proteins, and may help in the search for novel anti-adhesive drugs.

Introduction

Bacterial infection is often initiated by the adhesion of pathogens to host cells or tissues *via* surface-associated cell adhesion proteins.[1–4] With the advent of antibiotic-resistant strains, anti-adhesion therapy, which consists of blocking this interaction with soluble ligands, is emerging as a promising approach to treat infectious diseases.[5,6] However, designing efficient anti-adhesion drugs first requires a detailed understanding of the molecular bases of adhesion.

Mycobacterium species are known to adhere to the respiratory mucosa *via* fibronectin (Fn), a high-molecular weight glycoprotein found in the extracellular matrix, which binds to a wide variety of cell adhesion molecules.[7–10] Fn binding is highly conserved in mycobacteria.[11] Early studies revealed that Fn is involved in the adherence of *Mycobacterium bovis bacillus* Calmette-Guérin (BCG) to the bladder epithelium.[12–16] Other

Unité de Chimie des Interfaces, Université Catholique de Louvain, Croix du Sud 2/18, B-1348 Louvain-la-Neuve, Belgium.
E-mail: yves.dufrene@uclouvain.be; Fax: (+32) 10 47 20 05; Tel: (+32) 10 47 36 00

mycobacteria, including *Mycobacterium avium* complex (MAC) and *Mycobacterium tuberculosis*, have also been shown to bind to Fn, *via* fibronectin attachment proteins (FAPs) exposed on the bacterial cell surface.[16–19] *In vitro* studies have shown that peptides from the binding region of FAPs can block the attachment of mycobacteria to Fn.[11,18] Interestingly, the internalization of various species (*M. bovis* BCG, *M. leprae*, *M. avium*) by cultured epithelial cells is a FAP-dependent process. In addition, mycobacterial FAPs appear to play a role in cancer treatment. Intravesical *M. bovis* BCG is the treatment of choice for superficial bladder cancer.[20,21] There is growing evidence indicating that attachment of the mycobacteria to Fn within the bladder is necessary for mediation of the antitumor response.[21] Accordingly, elucidation of the molecular mechanisms underlying Fn attachment in mycobacteria is essential for understanding mycobacterial infections and mycobacterial antitumor activity.

Atomic force microscopy (AFM) has recently been established as a powerful technique for single-cell and single-molecule analysis, capable of observing the structures of live cells, measuring cell wall elasticity, exploring the conformational properties of surface polymers, and probing

---

Insight, innovation, integration

Studying the structure and function of bacterial cell adhesion proteins—referred to as adhesins—is essential given the important role they play in cellular processes and diseases, as well as their potential as drug targets. We have used *in vivo* single-molecule atomic force microscopy to explore the binding strength and surface distribution of fibronectin attachment proteins (FAPs) in *Mycobacterium bovis bacillus* Calmette-Guérin.

First, we mapped the distribution of individual FAPs, revealing that the proteins are widely exposed on the cell surface. Then, we showed that treatment of the bacterial cell walls with enzymes or antibiotics led to a substantial reduction of the FAP surface density, thus confirming that the proteins localize specifically on the outermost cell surface.
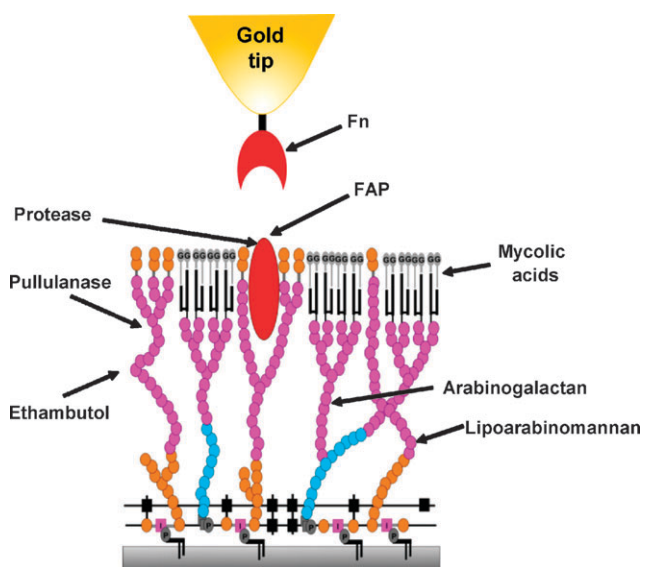
Fig. 1 A schematic representation of the experimental set-up, showing the Fn-modified AFM tip and the mycobacterial cell wall. The arrows indicate the major cell wall components and the action sites of the anti-mycobacterial drug, ethambutol (EMB), and of the enzymes pullulanase and protease.

the binding strength of cell adhesion molecules.[22,23] Here, we address the pertinent question as to whether AFM can localize FAP molecules on the surface of *M. bovis* BCG and measure their binding strength *in vivo* (Fig. 1).

Results and discussion

Design of Fn-tips

Measuring the interaction forces of cell surface receptors by AFM implies attaching a specific bioligand on the AFM tips using appropriate immobilization strategies.[22] Instead of attaching Fn using long spacer molecules, the proteins were directly attached to gold-coated tips *via* their sulfur atoms (Fig. 1). Indeed, each Fn monomer contains 29 disulfide bridges and two free cysteine groups, which are likely to bind strongly to gold. The question may be raised as to whether the attached Fn molecules remain functional and there are two arguments supporting this notion. First, given the large structure of Fn, it is reasonable to assume that at least a fraction of the bacterial-binding domains should be exposed in the solution, thus remaining functional and second, the same approach has been successfully used to measure Fn–FAP interactions in *Staphylococcus epidermis*.[24]

To assess the quality of the functionalized tips, model flat surfaces were modified in the same way and analyzed using AFM imaging in aqueous solution.[25] Fn-coated surfaces were rather smooth and stable upon repeated scanning, indicating that the proteins were well-attached (data not shown). To confirm the presence of protein layers, a small area was first recorded at large forces (>10 nN) for short periods of time, followed by imaging a larger portion of the same area under normal load. Imaging at high forces resulted in the grafted material being pushed aside, thereby revealing the underlying support. The thickness of the removed films

was found to be 2.3 ± 0.3 nm, confirming the presence of Fn on the surface.

AFM localizes FAPs on living mycobacteria

Fn-tips were used to detect FAPs on the surface of living mycobacteria immobilized on a polycarbonate membrane. As can be seen in Fig. 2A, topographic images revealed a smooth and homogeneous surface, consistent with earlier reports.[25] Fig. 2B and C show the adhesion force map and adhesion force histogram, together with representative force curves, recorded on the cell surface with a Fn-tip. In 63% of the cases, the curves showed either single or multiple binding forces. The distribution of the last adhesion forces, typically occurring at ~ 10–50 nm, showed a well-defined maximum at 52 ± 19 pN ($n = 1024$). Several observations suggest that the measured 50 pN adhesion forces reflect single Fn–FAP interactions. First, this value is in the range of values reported for single Fn–*S. epidermis*[24] and Fn–integrin[26] interactions, using similar recording conditions. Second, our adhesion forces are also close to those measured, on the same bacterial species, between the single mycobacterial adhesin HBHA (heparin-binding hemagglutinin) and heparin,[25] suggesting that forces in the 50 pN range are characteristic of single bacterial adhesins. Third, the occurrence of multiple interactions resulting from sample indentation is unlikely, given the very small applied forces (~ 400 pN) and the stiff bacterial cell
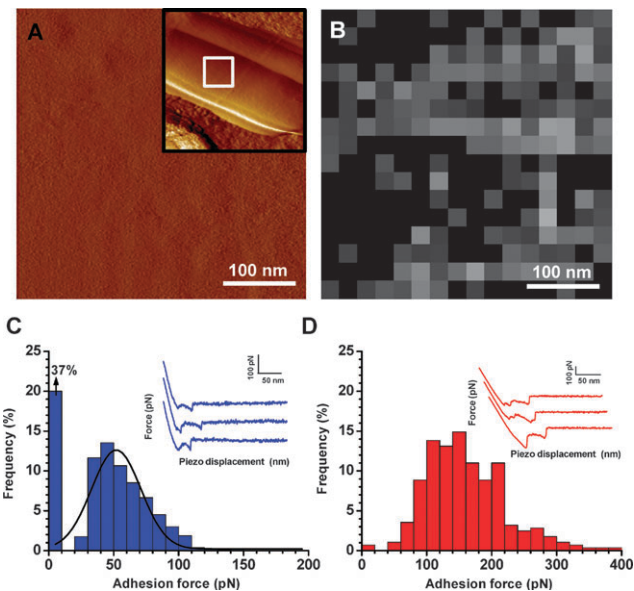

Fig. 2 The direct measurement of fibronectin (Fn)–fibronectin attachment protein (FAP) interactions in living *M. bovis* BCG. A: Low (inset; 2×2 μm) and high resolution deflection images of a living *M. bovis* BCG cell. B: The adhesion force map ($n = 256$ force curves taken in the square area in A; gray scale = 200 pN), and C: adhesion force histogram ($n = 1024$ force curves, taken from four force maps), together with representative force curves, recorded in PBS on the cell surface using a Fn-tip. Constant approach and retraction speeds (1000 nm s^{-1}) and interaction times (500 ms) were used. Similar data were obtained using more than ten different tips and ten different cells from independent cultures. D: The adhesion force histogram with representative force curves recorded after injecting a Fn solution on the cell surface.
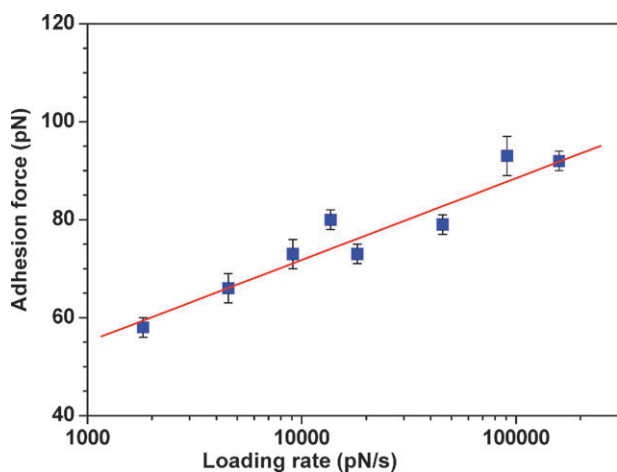
Fig. 3 The mean Fn–FAP adhesion force as a function of the loading rate. Force–distance curves were recorded in PBS between a Fn-tip and the *M. bovis* BCG surface. The data represent the mean ± s.e.m. ($n = 256$).

wall. Concerning the spatial arrangement of the FAPs on the cell surface, the adhesion maps (Fig. 2B) always revealed fairly homogeneous distributions, indicating that the proteins were widely and homogeneously exposed. We note that the smooth surface morphology (Fig. 2A) was not altered by the force measurements, thus supporting further the relevance of the force data.

In an attempt to demonstrate the specificity of the measured interaction, force curves were recorded after injection of a Fn solution on the cell preparation. As can be seen in Fig. 2D, treatment of the cell surface with Fn caused a dramatic increase of both the adhesion frequency and adhesion force values, which is the opposite of what we expect for a classical blocking experiment. We attribute this unusual behaviour to the occurrence of Fn–Fn interactions, consistent with the notion that this protein is known to self-associate to form aggregates and fibrils, a process directed by multiple binding sites that have been identified along the molecule.[8]

Receptor–ligand binding forces are known to depend on the rate at which the force is applied to the complex.[22,24,26,27] Therefore, we explored the dynamics of the Fn–FAP interaction by recording force curves at various loading rates (Fig. 3). We found that the mean adhesion force (F) increased linearly with the logarithm of the loading rate (r), as observed for Fn–*S. epidermis* interactions.[24] From these dynamic force spectroscopy data, the kinetic off-rate constant of dissociation at zero force was extracted, $k_{off} = 0.07$ s^{-1}, which is smaller than the 4.8 s^{-1} value determined for *S. epidermis*.[24]

Enzymes and antibiotics dramatically alter the FAP surface distribution

The mycobacterial cell wall has a highly complex organization (Fig. 1) and is essential for growth and survival in the infected host.[28,29] The cell wall is composed of crosslinked peptidoglycan linked to arabinogalactan, esterified at the distal ends to the mycolic acids. The other dominant feature is the lipoarabinomannan (LAM), somewhat embedded into the framework of the mycolylarabinogalactan, and anchored

into the cell membrane *via* its phosphatidylinositol portion, linked to a branched-chain arabinomannan polysaccharide. A variety of antibiotics target the biosynthesis of the *M. tuberculosis* cell wall,[29,30] including EMB, which inhibits the synthesis of the polysaccharidic portion of the envelope (arabinomannan and arabinogalactan). Besides antibiotics, enzymes may also target cell wall constituents. For instance, pullulanase cleaves α-(1-6) glucose polymers,[31] while proteases digest proteins, including cell-surface associated proteins.[32] Clearly, investigating the effects of drugs and enzymes on the mycobacterial envelope may provide novel information on its macromolecular architecture and assembly.

Here, pullulanase, protease and EMB were used to assess whether FAPs localize specifically on the cell surface or whether they are also found in the inner cell wall layers. First, we scanned the surface of mycobacteria in real-time with a Fn-tip, following injection of pullulanase (Fig. 4). Topographic imaging with increasing contact time demonstrated that the enzyme induced a substantial increase of roughness from 0.3 nm (root mean square roughness on 400 × 400 nm areas), to 1.8 nm after 1 h. Note that although the sequence of images was obtained in the same area, small drifts from one

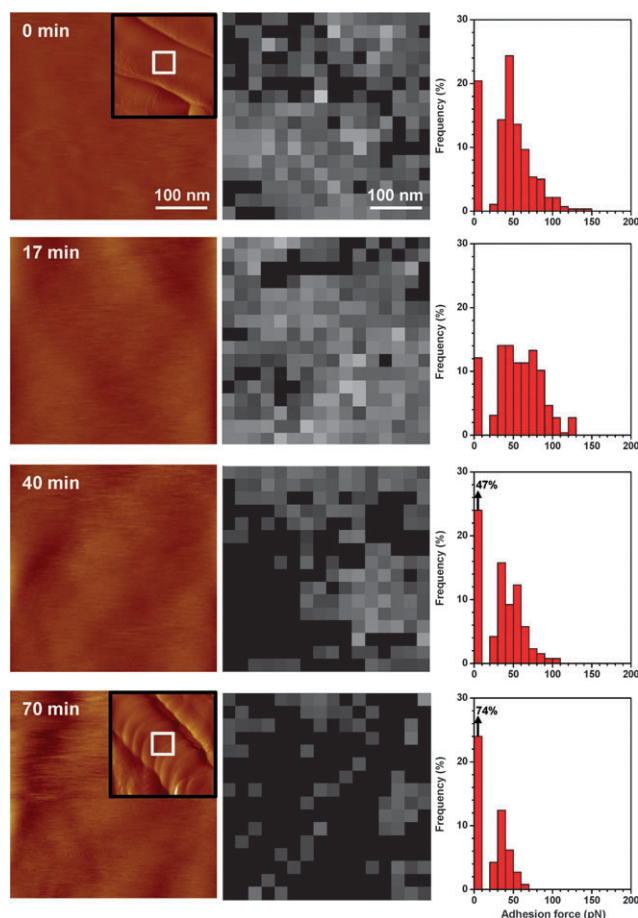**Fig. 4** Real-time alteration of the FAP distribution by pullulanase: low (insets; 2 × 2 μm) and high resolution images (left), and adhesion force maps (middle) and adhesion force histograms (right; $n = 256$) recorded on *M. bovis* BCG with a Fn-tip following incubation with pullulanase at 3.3 mg ml^{-1} for 0, 17, 40 and 70 min (from top to bottom, respectively).
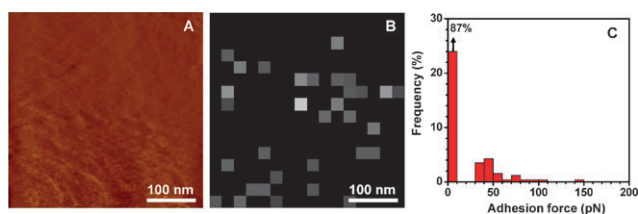
Fig. 5 Treatment with protease alters the FAP distribution. High-resolution image (left), adhesion force map (middle) and adhesion force histogram (right; $n = 256$) recorded on *M. bovis* BCG with a Fn-tip following incubation for 1 h with a 1 mg ml^{-1} solution of protease from *Streptomyces griseus*.
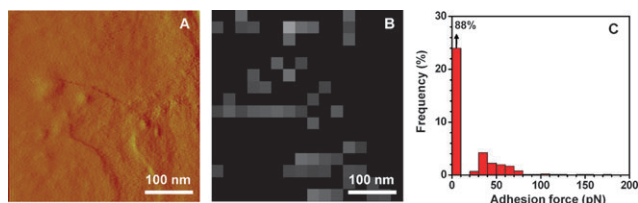

Fig. 6 Treatment with ethambutol alters the FAP distribution. High-resolution image (left), adhesion force map (middle) and adhesion force histogram (right; $n = 256$) recorded on *M. bovis* BCG with a Fn-tip following treatment for 24 h with ethambutol at 10 μg ml^{-1}.

image to another cannot be excluded. Besides these structural alterations, we also noted a strong reduction of the number of adhesion events, documenting a reduction of the FAP density.

Then, we examined cells pre-treated with a protease solution for 1 h, and we also found an increase in cell surface roughness and a reduction of adhesion frequency (from 63% to 13%) (Fig. 5). As opposed to the pullulanase experiments, measurements at 0 min (no treatment) are not available, since the cells were not imaged in real-time. Thus, the data should be compared to those of Fig. 2. Lastly, when cells were pre-incubated with EMB, major structural changes were also observed, consistent with earlier studies.[33,34] In addition, only 12% of the curves showed adhesion events, with no clear maximum being observed in the adhesion force distribution (Fig. 6). Hence, the above analyses reveal that both the enzymes and the drug induced major cell surface alterations, presumably reflecting the removal of outer cell wall layers, together with a substantial reduction of the FAP surface density. This finding supports the notion that FAPs localize specifically on the outermost surface of mycobacteria.

Conclusion

In summary, this study reports on the first direct measurement of Fn–FAP interactions in mycobacteria using *in vivo* AFM. Our data demonstrate that FAPs decorate the entire surface of *M. bovis* BCG and that their binding strength is in the range of that reported for cell adhesion proteins. Treatments with pullulanase, protease and EMB all led to substantial alteration of the cell surface and reduction of the FAP surface density, revealing that FAPs localize specifically on the cell surface. An exciting challenge for future work is to determine whether the above findings also apply to other mycobacterial species, particularly MAC and *M. tuberculosis*. Also of interest would

be to compare the efficiency of a series of anti-adhesion molecules, *i.e.* molecules that block Fn attachment.

Experimental

Bacterial cultures

Mycobacterium bovis bacillus Calmette Guérin (BCG) (strain 1173P2, World Health Organization, Stockholm, Sweden) was grown in Sauton medium as described elsewhere.[35] Mycobacteria were cultured at 37 °C for about 10 d (OD$_{600}$ ∼0.6) in static conditions using 75 cm^2 Roux flasks that contained 50 mL of Sauton medium. For ethambutol experiments, cells were resuspended for 24 h in Sauton medium containing the antibiotic at the concentration corresponding to minimum inhibitory concentration (10 μg ml^{-1}).

Preparation of fibronectin-modified tips

Fibronectin was bound onto gold-coated AFM tips by sulfur–gold bonds. AFM cantilevers (Microlevers, Veeco Metrology Group, Santa Barbara, CA) were coated using electron beam thermal evaporation with a 5 nm thick Cr layer followed by a 30 nm thick Au layer. Before use, the gold-coated cantilevers were rinsed with ethanol, dried with a gentle nitrogen flow and cleaned for 5 min by UV/ozone treatment (Jelight Co., Irvine, CA). They were immersed overnight in PBS containing 10 μg ml^{-1} fibronectin and further rinsed several times with PBS.

AFM measurements

AFM images and force–distance curves were obtained in PBS solution (10 mM PBS, 150 mM NaCl, pH 7.4) at room temperature, using a Nanoscope IV Multimode AFM (Veeco Metrology Group, Santa Barbara, CA). *Mycobacterium bovis bacillus* Calmette Guérin (BCG) were harvested by centrifugation, washed three times with deionized water, and resuspended to a concentration of ∼10^8 cells mL^{-1}. To image mycobacteria in their native state by AFM, the cells were immobilized onto porous polycarbonate membranes (Millipore), with a pore size of 1.2 μm. This approach is well suited to image single cells under aqueous conditions and it does not involve chemical treatment or drying, which would cause rearrangement or denaturation of the surface molecules. After filtering a concentrated cell suspension, the filter was gently rinsed with deionized water, carefully cut (1 × 1 cm), attached to a steel sample puck (Veeco Metrology Group) using a small piece of adhesive tape and the mounted sample was transferred into the AFM liquid cell while avoiding dewetting. For the blocking experiment, the sample was briefly incubated with a 10 μg ml^{-1} of Fn, then rinsed with PBS. For the pullulanase experiments, 2 μl of a 3.3 mg ml^{-1} solution of pullulanase (Sigma) were injected on the mounted sample. For the protease experiments, the sample was incubated for 1 h with a 1 mg ml^{-1} solution of protease from *Streptomyces griseus* (Sigma), then rinsed with PBS and transferred into the AFM liquid cell. For SMFS measurements, all curves were recorded with a maximum applied force of ∼400 pN. To estimate the spring constants of the cantilevers (∼0.011 N m^{-1}), we

measured their geometrical dimensions using scanning electron microscopy, as well as their free resonance frequency.

Acknowledgements

References

1 C. R. Hauck, F. Agerer, P. Muenzner and T. Schmitter, *Eur. J. Cell Biol.*, 2006, **85**, 235–242.
2 B. B. Finlay and P. Cossart, *Science*, 1997, **276**, 718–725.
3 K. J. Verstrepen, T. B. Reynolds and G. R. Fink, *Nat. Rev. Microbiol.*, 2004, **2**, 533–540.
4 J. L. Telford, M. A. Barocchi, I. Margarit, R. Rappuoli and G. Grandi, *Nat. Rev. Microbiol.*, 2006, **4**, 509–519.
5 J. Beuth, B. Stoffel and G. Pulverer, *Adv. Exp. Med. Biol.*, 1996, **408**, 51–56.
6 N. Sharon and I. Ofek, *Glycoconjugate J.*, 2000, **17**, 659–664.
7 S. N. Abraham, E. H. Beachey and W. A. Simpson, *Infect. Immun.*, 1983, **41**, 1261–1268.
8 R. Pankov and K. M. Yamada, *J. Cell Sci.*, 2002, **115**, 3861–3863.
9 D. Joh, E. R. Wann, B. Kreikemeyer, P. Speziale and M. Höök, *Matrix Biol.*, 1999, **18**, 211–223.
10 U. Schwarz-Linek, J. M. Werner, A. R. Pickford, S. Gurusiddappa, J. H. Kim, E. S. Pilka, J. A. G. Briggs, S. Gough, M. Höök, I. D. Campbell and J. R. Potts, *Nature*, 2003, **423**, 177–181.
11 J. Schorey, Q. Li, D. McCourt, M. Bong-Mastek, J. Clark-Curtiss, T. Ratliff and E. Brown, *Infect. Immun.*, 1995, **63**, 2652–2657.
12 M. J. Becich, S. Carroll and T. L. Ratliff, *J. Urol.*, 1991, **145**, 1316–1324.
13 K. Kuroda, E. J. Brown, W. B. Telle, D. G. Russell and T. L. Ratliff, *J. Clin. Invest.*, 1993, **91**, 69–76.
14 T. L. Ratliff, R. McCarthy, W. B. Telle and E. J. Brown, *Infect. Immun.*, 1993, **61**, 1889–1894.
15 D. L.-W. Cheng, W.-P. Shu, J. C. S. Choi, E. J. Margolis, M. J. Droller and B. C. S. Liu, *J. Urol.*, 1994, **152**, 1275–1280.
16 A. M. Middleton, M. V. Chadwick, A. G. Nicholson, A. Dewar, R. K. Groger, E. J. Brown and R. Wilson, *Mol. Microbiol.*, 2000, **38**, 381–391.
17 S. P. Rao, K. R. Gehlsen and A. Catanzaro, *Infect. Immun.*, 1992, **60**, 3652–3657.
18 J. S. Schorey, M. A. Holsti, T. L. Ratliff, P. M. Allen and E. J. Brown, *Mol. Microbiol.*, 1996, **21**, 321–329.
19 W. Zhao, J. S. Schorey, R. Groger, P. M. Allen, E. J. Brown and T. L. Ratliff, *J. Biol. Chem.*, 1999, **274**, 4521–4526.
20 A. Morales, D. Eidinger and A. Bruce, *J. Urol.*, 1976, **116**, 180–183.
21 W. Zhao, J. S. Schorey, M. Bong-Mastek, J. Ritchey, E. J. Brown and T. L. Ratliff, *Int. J. Cancer*, 2000, **86**, 83–88.
22 P. Hinterdorfer and Y. F. Dufrêne, *Nat. Methods*, 2006, **3**, 347–355.
23 Y. F. Dufrêne, *Nat. Rev. Microbiol.*, 2008, **6**, 674–680.
24 Y. Bustanji, C. R. Arciola, M. Conti, E. Mandello, L. Montanaro and B. Samori, *Proc. Natl. Acad. Sci. U. S. A.*, 2003, **100**, 13292–13297.
25 V. Dupres, F. D. Menozzi, C. Locht, B. H. Clare, N. L. Abbott, S. Cuenot, C. Bompard, D. Raze and Y. F. Dufrêne, *Nat. Methods*, 2005, **2**, 515–520.
26 F. Li, S. D. Redick, H. P. Erickson and V. T. Moy, *Biophys. J.*, 2003, **84**, 1252–1262.
27 R. Nevo, C. Stroh, F. Kienberger, D. Kaftan, V. Brumfeld, M. Elbaum, Z. Reich and P. Hinterdorfer, *Nat. Struct. Biol.*, 2003, **10**, 553–557.
28 P. J. Brennan, *Tuberculosis*, 2003, **83**, 91–97.
29 P. J. Brennan and D. C. Crick, *Curr. Top. Med. Chem.*, 2007, **7**, 475–488.
30 D. Chatterjee, *Curr. Opin. Chem. Biol.*, 1997, **1**, 579–588.
31 P. Dinadayala, A. Lemassu, P. Granovski, S. Cerantola, N. Winter and M. Daffé, *J. Biol. Chem.*, 2004, **279**, 12369–12378.
32 F. Ahimou, A. Touhami and Y. F. Dufrêne, *Yeast*, 2003, **20**, 25–30.
33 C. Verbelen, V. Dupres, F. D. Menozzi, D. Raze, A. R. Baulard, P. Hols and Y. F. Dufrêne, *FEMS Microbiol. Lett.*, 2006, **264**, 192–197.
34 D. Alsteens, C. Verbelen, E. Dague, D. Raze, A. R. Baulard and Y. F. Dufrêne, *Pfluegers Arch.*, 2008, **456**, 117–125.
35 F. D. Menozzi, J. H. Rouse, M. Alavi, M. Laude-Sharp, J. Muller, R. Bischoff, M. J. Brennan and C. Locht, *J. Exp. Med.*, 1996, **184**, 993–1001.